Pergamon

Tetrahedron 55 (1999) 5741–5758

TETRAHEDRON

Aminoglycoside Hybrids as Potent RNA Antagonists

Jeffrey B.-H. Tok, Junhyeong Cho & Robert R. Rando*

Department of Biological Chemistry and Molecular Pharmacology, Harvard Medical School

250 Longwood Avenue, Boston, MA 02115, USA

Received 31 July 1998; revised 6 March 1999; accepted 11 March 1999

Abstract: Aminoglycosides specifically bind to the A-site decoding region of prokaryotic 16S rRNA with dissociation constants in the 1-2 μM range. The aminoglycoside paromomycin binds to a truncated A-site construct with a K_d = 1.85 μM. Paromomycin analogs are described here in which the aminoglycoside is linked via spacer groups to either thiazole orange or pyrene. These analogs bind specifically to the truncated A-site construct, but with affinities considerably higher than paromomycin itself. The binding of the hybrid molecules to the A-site is greater the shorter the spacer group.

Keywords: Aminoglycosides, fluorescence, 16S ribosomal RNA, hybrid, antagonists.

INTRODUCTION

RNA molecules possess well defined three dimensional structures which to that can bind small molecules with great specificity and with high affinities[1]. The aminoglycoside antibiotics comprise one set of molecules which bind to RNA molecules and exert their biological action by binding to particular RNA molecules[2,3]. The aminoglycosides act as antibacterial agents by binding to a particular region of the prokaryotic 16S rRNA causing mistranslation of message and premature termination of message[4,5]. The aminoglycoside binding site, the A-site of the decoding region, is involved in mediating interactions between mRNA, rRNA, and aminoacyl tRNAs[6].

While the 16S rRNA is too large to study mechanistically, recent studies have demonstrated that it can be simplified while still retaining biochemical function. Mini decoding region constructs containing 49 nts[7], 27 nts[8], and 129 nts[9] have been prepared and all of them show predicted biochemical activities. The 129 nt construct, which contains both the A and P-sites, binds aminoglycosides stoichiometrically at the A-site and with predicted affinities, generally in the low μM range[9]. In this instance, binding was determined by a quantitative fluorescence anisotropy method in which carboxy-tetramethylrhodamine labeled paramomycin, CRP (Scheme 1), was utilized

* To whom correspondence should be addressed. E-mail:rando@warren.med.harvard.edu

0040-4020/99/$ - see front matter
PII: S0040-4020(99)00240-9

as the probe[9]. Interestingly, CRP bound to the rRNA construct with an approximately 11-fold higher affinity than did paromomycin itself, suggesting that the aromatic rhodamine moiety interacts with the RNA[9]. It was also

Scheme 1. Structures of Paromomycin and CRP.

(Legend: Paromomycin, X = H; CRP, X = Carboxy-tetramethylrhodamine)

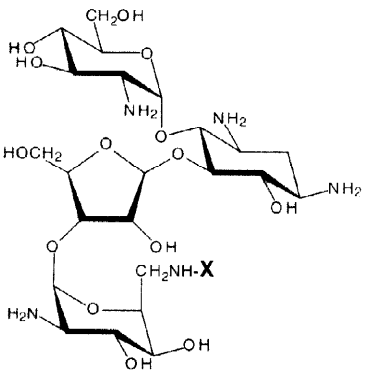

X = H **Paramomycin**

X = 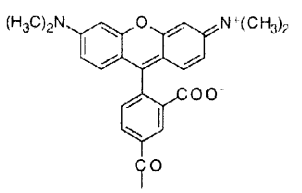

CRP

observed that a tobramycin pyrene conjugate had a higher affinity for tobramycin binding aptamers than did tobramycin itself[10]. These studies suggest that aminoglycoside conjugates containing intercalating agents might bind to RNA targets with higher affinities than do aminoglycosides by themselves. Since aminoglycosides bind relatively weakly to their bacterial targets and present dose-limiting nephro and ototoxicities[11,5], it is of some interest to discover more potent derivatives of these drugs. In this article, binding of aminoglycoside conjugates to an A-site decoding region construct is explored. Paromomycin conjugates of pyrene and thiazole orange, two putative intercalating agents, bind to the A-site construct with significantly higher affinities than does paromomycin itself. There is an important dependence of binding affinity on the length of the linker between paromomycin and the intercalator. Conjugates with shorter linkers exhibit higher affinities.

Figure 1. The secondary structure of the 27 nt A-site 16S rRNA construct as reported by Fourmy et al.[8] Paromomycin binds to the internal loop of the construct. The double mutant 16S rRNA construct has the internal loop removed.

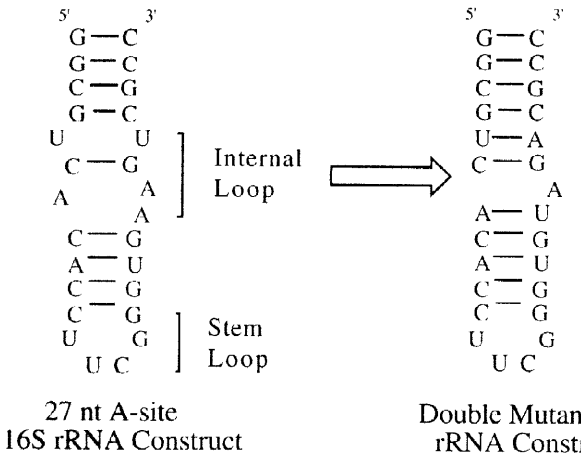

Scheme 2: Synthetic schemes for the synthesis of paramomycin-thiazole orange conjugate molecule **1**. The procedures outlined are applied to the synthesis of other paramomycin-thiazole orange conjugate molecules with carbon linkers of different length (**2** - **5**).

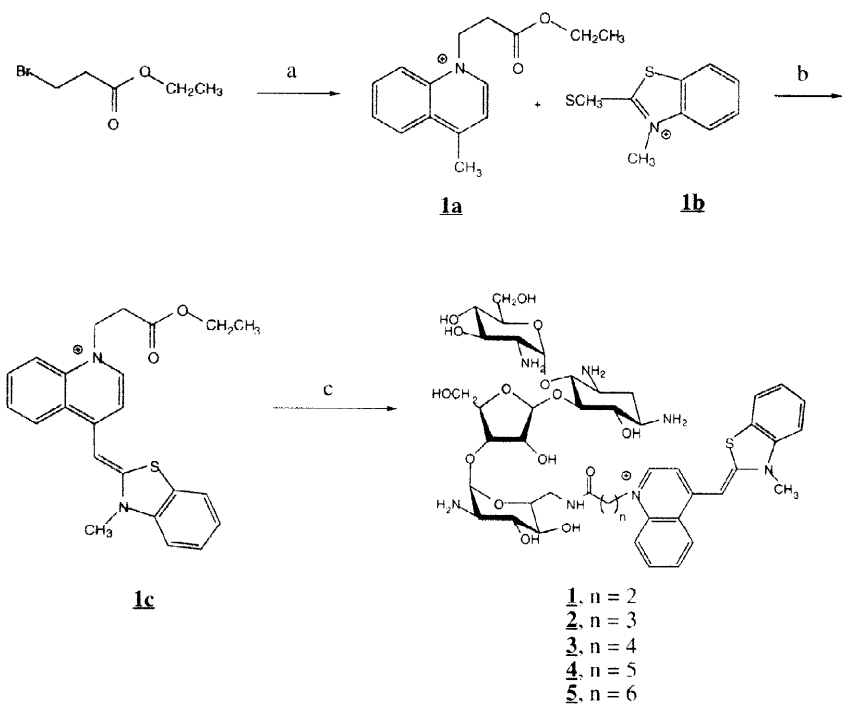

Conditions : (a) (i) NaI, acetone, reflux; (ii) lepidine, dioxane, reflux; (b) Et_3N, EtOH; (c) (i) 1:1 2N NaOH/dioxane; (ii) HOBT, DCC, paramomycin sulfate, DMF.

Figure 2. Fluorescence anisotropy of CRP (10 nM) containing the A-site 16S rRNA construct (300 nM) of the paramomycin-thiazole orange conjugate molecules **1** - **5**.

(A) Compound **1**:

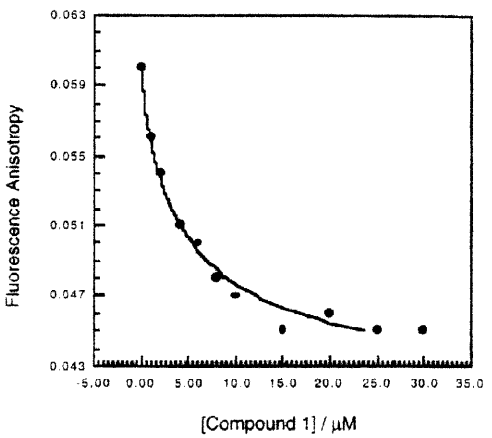

(B) Compound **2**:

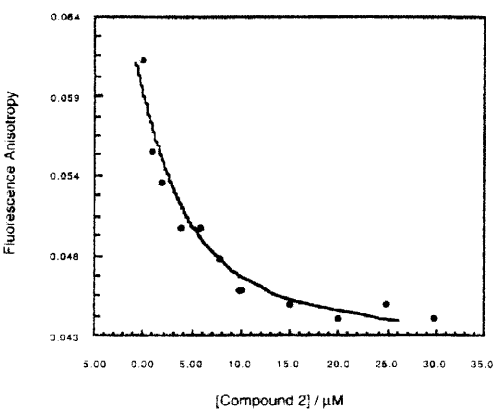

(C) Compound **3**:

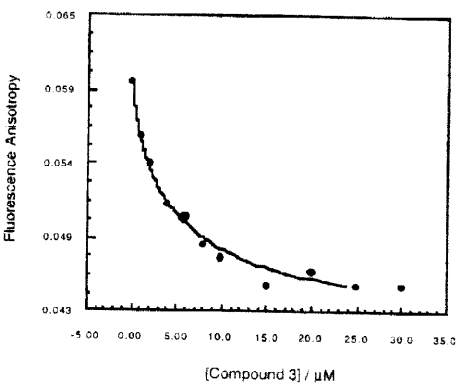

(D) Compound **4**:

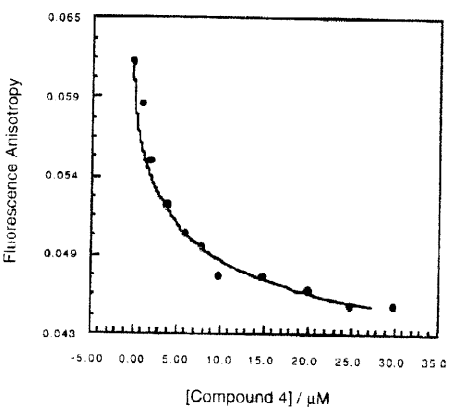

(E) Compound **5**:

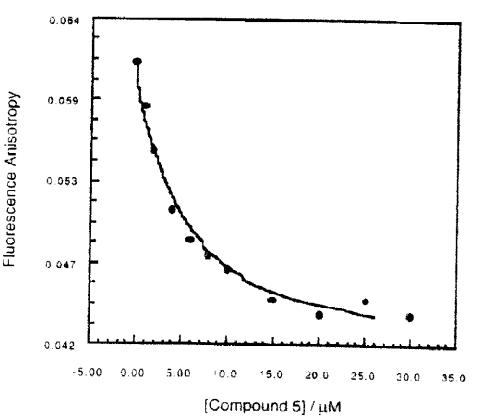

RESULTS

(A) *The Binding of Paromomycin-Thiazole Orange Conjugates to an A-Site Decoding Region Construct*

In the experiments described here the 27 nt A-site construct[8] was chosen for study as it is the simplest and least expensive construct to prepare (Figure 1). This construct is well-behaved with respect to aminoglycoside binding and binds the aminoglycosides paromomycin and CRP with dissociation constants of 1.87 μM and 0.21 μM respectively (Tok, J.; Cho, J.; Rando, R. R.-unpublished experiments). The five thiazole orange analogs (**1** - **5**) shown in Scheme 2 were prepared and tested as competitors of CRP binding to the A-site construct. These measurements are performed by following the decrease in anisotropy of RNA-CRP complex as a function of analog concentration[9]. The experimentally determined points are plotted along with a theoretical line for stoichiometric binding[9,10]. Overlap of the points and the line provides evidence for stoichiometric binding and the dissociation constants (K_d) can be readily calculated from the curve.

Table 1. Binding constants of the paramomycin-thiazole orange conjugate molecules **1** - **5** against the 27 nt A-site 16S rRNA construct.

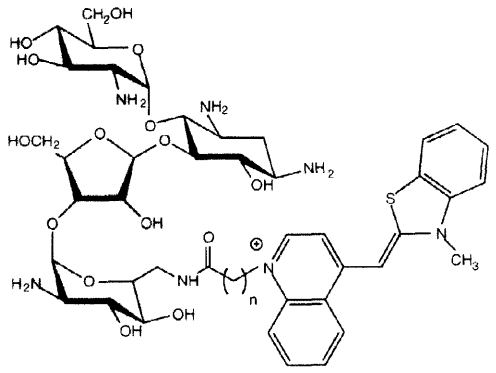

Aminoglycoside derivatives		K_d / nM
1	n = 2	46.46 ± 8.71
2	n = 3	49.32 ± 4.56
3	n = 4	193.43 ± 52.20
4	n = 5	456.92 ± 92.64
5	n = 6	470.05 ± 72.15

Scheme 3: Synthetic schemes for the synthesis of paramomycin-pyrene conjugate molecule **6**. The procedure outlined are applied to conjugate molecules **7** - **10**.

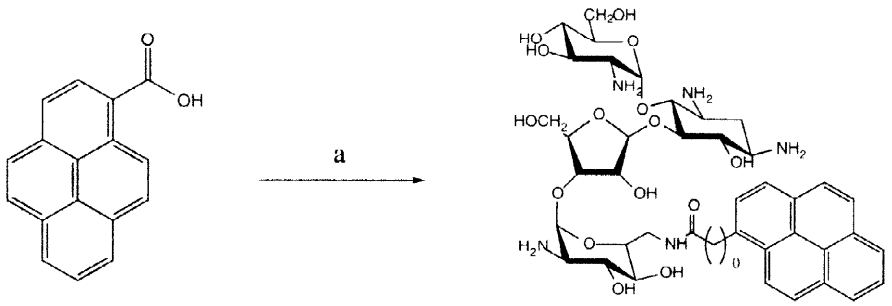

6, n = 0
7, n = 1
8, n = 3
9, n = 5
10, n = 9

Conditions : (a) (i) DCC, N-hydroxysucciimide, DMF; (ii) paramomycin sulfate, dioxane.

Table 2. Binding constant of the paromomycin-pyrene conjugate molecules **6** - **10** against the 27 nt A-site 16S rRNA construct.

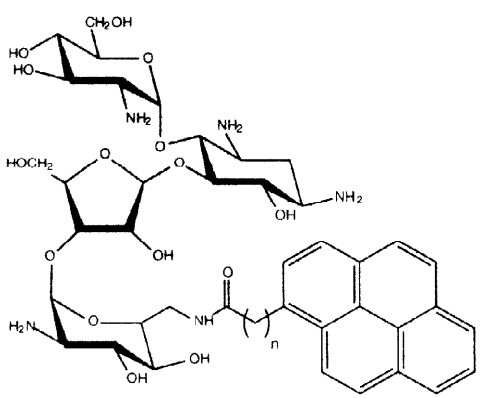

Aminoglycoside derivatives		K_d / nM
6	n = 0	213 ± 20
7	n = 1	245 ± 16
8	n = 3	277 ± 36
9	n = 5	1784 ±46
10	n = 9	1987 ± 63

The data for compounds are shown in Figure 2 A-E, and the calculated dissociation constants are provided in Table 1. The experimentally determined points fit the curves for stoichiometric binding quite well. It is noteworthy that the binding affinities increase as the spacer chain length decreases. It is interesting to note that analog **1** binds to the decoding region with an appreciable affinity for the decoding region (46 nM) which to that is approximately 41-fold greater than for paromomycin itself. The fall off in binding affinity as a function of spacer chain length suggests weak interactions between the thiazole orange and RNA which to that rapidly dissipate as the aromatic moiety is moved away from the RNA.

(B) *The Binding of Paromomycin-Pyrene Conjugates to an A-Site Decoding Region Construct*

To determine whether the same pattern of binding would be observed with a different putative intercalating moiety, binding studies were performed with the paromomycin-pyrene conjugates (**6** - **10**) shown in Scheme 3. Since these analogs are fluorescent and the fluorescence is quenched upon binding to the RNA receptor[10], direct fluorescence quenching studies could be performed with the analogs. As shown in Figure 3 A-E, a similar pattern of binding behavior was observed with the pyrene conjugates as was observed with the thiazole orange conjugates, except the binding enhancements were smaller for the paromomycin-pyrene conjugates and no binding enhancements were observable at the longer spacer chain lengths. The calculated dissociation constants are provided in Table 2. In order to demonstrate that the binding of paromomycin hybrids to the A-site construct is specific, a double mutant of this construct was prepared (Figure 1) and studied with respect to its ability to bind to the paromomycin-pyrene conjugates. This double mutant would neither be expected to bind to paromomycin[8,11] nor to the hybrid molecules. As shown in Figure 4 A-E, weak and non-specific binding was observed with the various analogs, which probably involves weak interactions with the pyrene moieties.

DISCUSSION

In the experiments reported here novel aminoglycoside conjugates, containing putative intercalating agents, were prepared and studied as ligands for an A-site decoding region construct. Like other constructs of this type[2], the 27-nt A-site decoding region construct specifically binds aminoglycosides. In fact, high field NMR experiments on this decoding region construct, bound to the aminoglycoside paromomycin, have been performed, and reveal important contacts made between the aminol moieties of the A, B rings of the aminoglycoside and the RNA[8]. Most aminoglycosides bind to A-site with affinities in the 1-2 μM range[7-9]. Neomycin is the exception

Figure 3. Relative fluorescence intensity of paramomycin-pyrene conjugate molecule **6** - **10** (10 nM) as a function of the A-site 16S rRNA construct. i refers to fluorescence intensity with the addition of the paramomycin-pyrene conjugate molecule, and io refers to the fluorescence intensity without the addition of the paramomycin-pyrene conjugate molecule.

(A) Compound **6**:

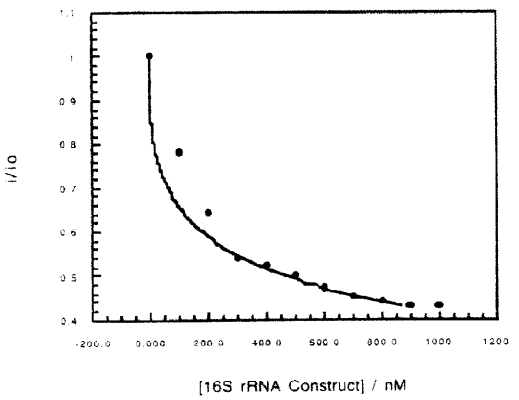

(B) Compound **7**:

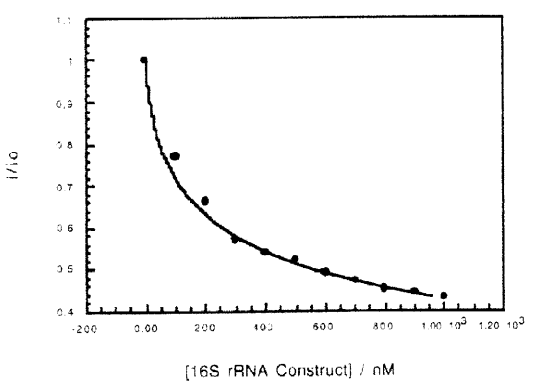

(B) Compound **8**:

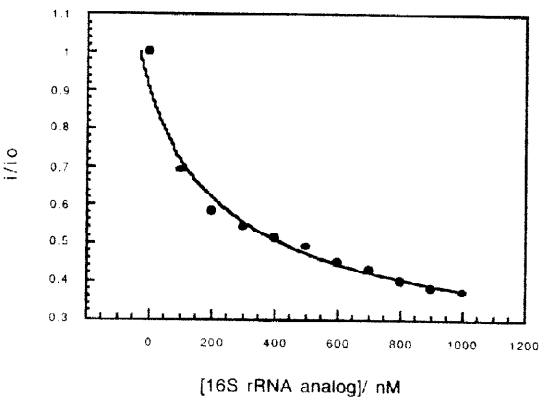

(C) Compound **9**:

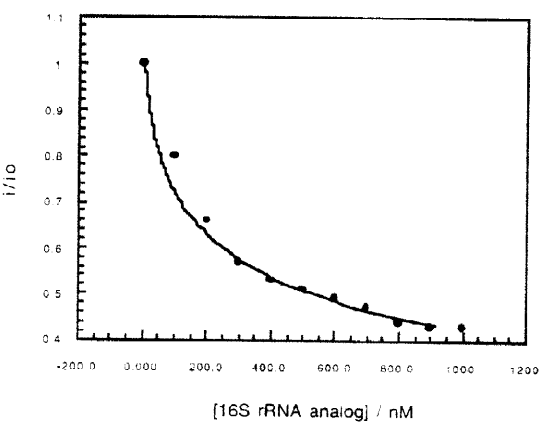

(D) Compound **10**:

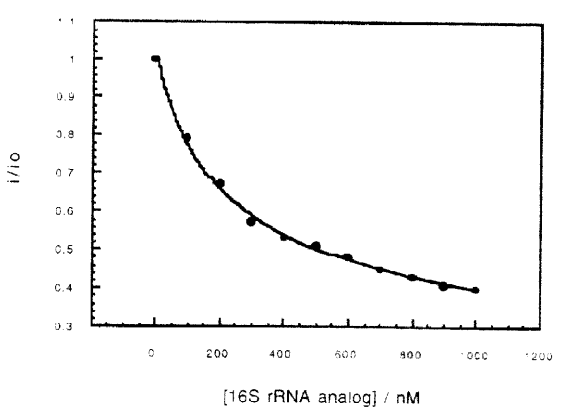

Figure 4. Relative fluorescence intensity of paramomycin-pyrene conjugate molecule **6** - **10** (10 nM) as a function of the double mutant A-site 16S rRNA construct (Figure 1). i refers to fluorescence intensity with the addition of the paramomycin-pyrene conjugate molecule, and io refers to the fluorescence intensity without the addition of the paramomycin-pyrene conjugate molecule.

(A) Compound **6**:

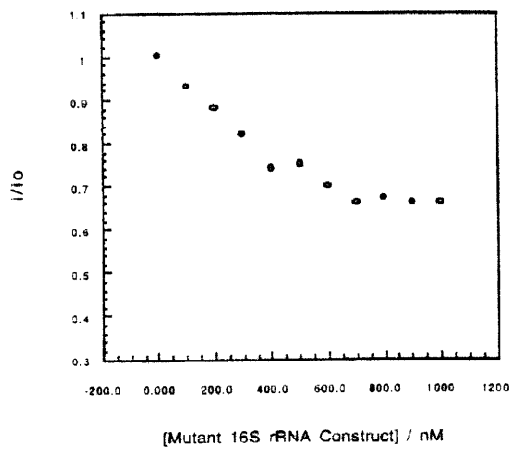

(B) Compound **7**:

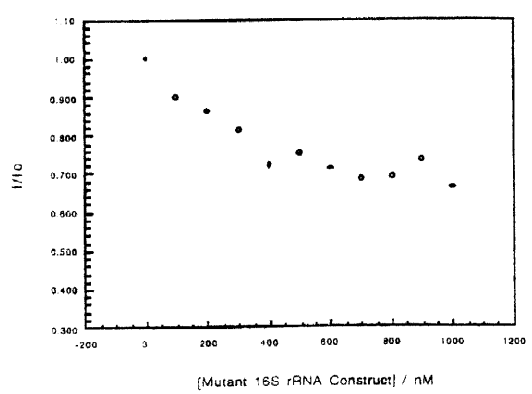

(C) Compound **8**:

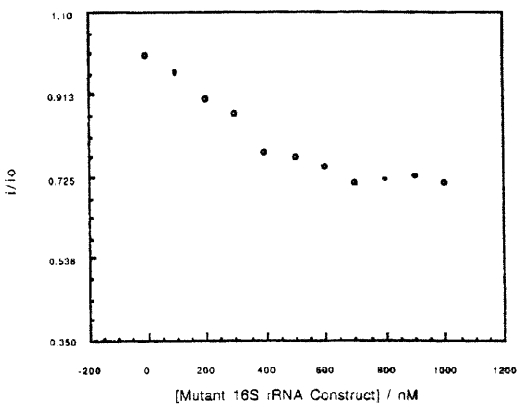

(D) Compound **9**:

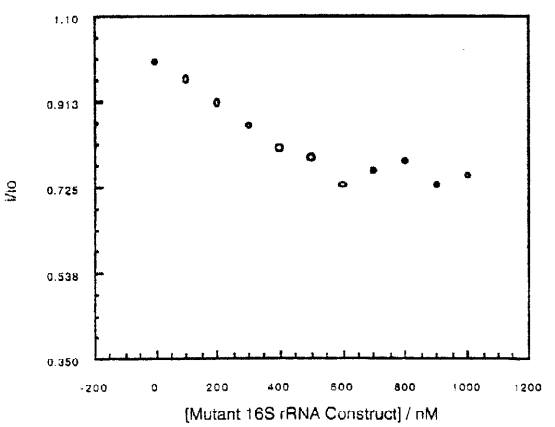

(E) Compound **10**:

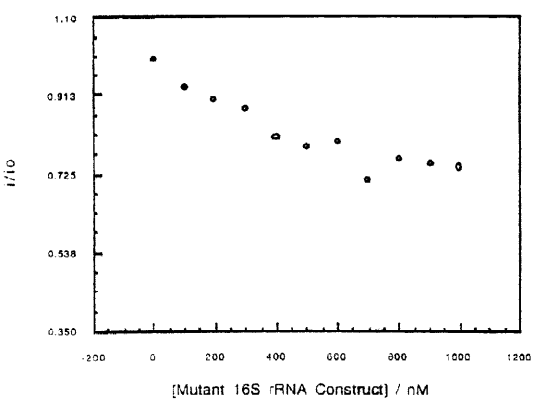

with a $K_d = 0.2\ \mu M$[9]. These relatively modest affinities require high dose clinical use of aminoglycosides which leads to nephrotoxicity and ototoxicity[11]. It would therefore be of substantial interest to design aminoglycosides with enhanced affinities for the A-site with the hope that these analogs would avoid high dose related toxicities. It had been previously noticed that fluorescently labeled aminoglycosides, used for quantitatively measuring binding constants of aminoglycoside binding RNA molecules, bound to the RNA molecules with higher affinities than did the unconjugated aminoglycosides[9,10]. This clearly suggests that the fluorescence probe is interacting with the RNA molecule and immediately suggests a device to enhance aminoglycoside affinities for the decoding region.

In the current study, aminoglycoside conjugates with the nucleic acid intercalators pyrene[13] and thiazole orange[14,15] have been prepared, and studied as ligands for the A-site construct. One of the paromomycin thiazole orange analogs **3** bound stoichiometrically to the construct with a K_d = 46 nM. This is the highest published affinity of any ligand, aminoglycoside or otherwise, to the A-site. This molecule binds to the A-site with a 41-fold higher affinity for the A-site than does paromomycin itself. Interestingly, the affinities of the paromomycin-thiazole orange adducts for the A-site fell off substantially as the spacer length distance between the thiazole and aminoglycoside moieties is increased. This suggests a relatively weak affinity for thiazole orange and RNA which is readily diluted by entropic factors due to the flexibility of the linker. Still, the lowest affinity antagonist in this series **5** bound to the A-site with an approximately 4-fold higher affinity for the A-site than paromomycin.

Generally weaker affinities were found in the pyrene series of adducts **6** - **10**. Here, the fall off in binding affinities with spacer chain length proved to be rather abrupt. Analogs **9** and **10** had approximately the same affinities for the A-site as did paromomycin itself, suggesting that the pyrene moiety was no longer interacting with the RNA molecule. We had previously found that pyrene has a relatively weak affinity, in the low mM range, for RNA molecules (Wang, Y.; Rando, R. R.-unpublished experiments). Therefore, under the best of conditions where the paromomycin and pyrene both bound to the RNA molecule in an independent and additive fashion, we might expect to observe affinities in the 10 nM range. The studies described are qualitatively consistent with this approximation. The best pyrene analog bound with a K_d = 213 nM, which suggests that pyrene has only a weak affinity for the A-site. The fact that the thiazole orange analogs had a higher affinity for the A-site would imply that thiazole orange might have a higher affinity for this RNA construct than does pyrene.

Many different aromatic containing ligands (both organic cations and intercalators), including berenil[16], 4',6-diamino-2-phenylindole (DAPI)[17], 2-phenylquinoline[18], diphenylfuran derivatives[19], polycationic ligands[20], ethidium[21], and acridine[21], have been tested for their abilities to interact with RNA molecules. Of these the most high affinity ligands appear to be the diphenylfuran derivatives. We have not synthesized paromomycin analogs containing the high affinity RNA intercalating agents yet, but it would be presumed that their affinities for the A-

site construct would be higher than those reported here with the modestly binding intercalators. However, specificity of binding is as important as high affinity is. The adducts reported here appear to exhibit specific affinity for the A-site bulge structure because the double A-site mutant investigated, in which the bulge is abolished, did not specifically bind the pyrene-paromomycin adducts. It is known that paromomycin binding to the A-site importantly involves bulge recognition[8]. Thus, the binding of the adducts to the A-site is driven by paromomycin A-site interactions. It will be interesting to determine if paromomycin adducts with higher affinity RNA intercalators will still be highly specific for the A-site. Intercalating agents highly specific for particular RNA structures are not readily available[1]. However, as more specific intercalating, or just hydrophobic analogs, are designed to recognize particular RNA structures, either through stacking or hydrophobic interactions, it should be possible to formulate hybrid aminoglycoside containing analogs with high affinities and specificities for particular RNA structures. One thing that is clear from the studies reported here is that the affinities of aminoglycosides for the decoding region A-site can be adjusted upward by generating hybrids of these analogs with molecules of only modest affinities for RNA. These hybrid molecules still maintain the specificity of the parent aminoglycoside, but have substantially higher affinities than does the parent. Further studies with these hybrids will determine if high selectivities of action can be maintained as target affinities become extremely high.

EXPERIMENTAL SECTION

Materials and Methods. Ethyl 3-bromopropionate, ethyl 4-bromobutyrate, ethyl 5-bromovalerate, ethyl 6-bromohexanoate, ethyl 7-bromoheptanoate were purchased from Aldrich Chemical Company (Milwaukee, WI). 1-Pyrenecarboxylic acid, 1-pyreneacetic acid, 1-pyrenebutanoic acid, 1-pyrenehexanoic acid and 1-pyrenedecanoic acid were purchased from Molecular Probes (Eugene, OR). Paramomycin sulfate was purchased from Sigma (St. Louis, MO). All chemicals were used without further purification. The 27 nt A-site 16S rRNA construct was purchased from Oligos Etc. (Wilsonville, OR). All stock solution were prepared in water.

Proton (^{1}H) and ^{13}C nuclear magnetic resonance (NMR) spectra were obtained with a Varian VRX 500S spectrometer operating at a proton frequency of 499.843 MHz. The residual proton absorption of the deuterated solvent ($CDCl_3$ or D_2O) was used as the internal standard. All ^{1}H and ^{13}C NMR chemical shifts are reported as δ values in parts per million (ppm), and the coupling constants (J) are given in hertz. The splitting pattern abbreviations are as follows: s, singlet; d, doublet; t, triplet; q, quartet; br, broad; m, multiplet; dd, doublet of doublets. For spectrophotometer measurements, a Perkin-Elmer Lambda 3B UV/Vis spectrophotometer was employed. HR (High Resolution) and FAB (fast atom bombardment) mass spectra was performed in a JEOL

mass spectrometer JMS-SX102. Analytical and preparative HPLC was conducted on a Waters 625 LC system with UV detection. The columns used were a Rainin ODS C18 5 X 26 mm analytical column (100 Å) or a semi-preparative Dynamax C18 column (300 Å).

Synthesis of the Paramomycin-Thiazole Orange Conjugates. The synthetic procedures for the various paramomycin- thiazole orange conjugates are similar. Hence the synthetic procedures for only the paramomycin-thiazole orange conjugate **1** is given in detail.

Compound 1a. In a solution of NaI (6.54 g, 43.6 mmoles) in anhydrous acetone, ethyl 3-bromopropionate (7.30 g, 34.9 mmoles) was added in one portion and stirred at room temperature for 30 min. The mixture was then refluxed for 30 min, and cooled to room temperature. The residue formed was filtered, and washed with acetone. The organic solution was collected and evaporated *in vacuo* to afford ethyl 3-iodopropionate in 94% yield.

Ethyl 3-iodopropionate (34.9 mmoles) was added to a solution mixture of lepidine (1.0 g, 6.98 mmoles) in 10 mL of dioxane. The solution was refluxed for 12 h. After cooling to room temperature, 30 mL of water was added to quench the reaction. The mixture was extracted three times with EtOAc (2 volumes). The organic phase was collected, washed once with water and brine, and dried over anhydrous Na_2SO_4. The organic solvent was evaporated *in vacuo* and chromatographed to afford the product **1a** in 81% yield. ^{1}H-NMR (in $CDCl_3$, 500 MHz) δ = 1.26 (t, 3H, J = 7.1 Hz), 2.54 (t, 2H, J = 5.3 Hz), 3.07 (s, 3H), 4.21 (q, 2H, J = 6.9 Hz), 5.38 (t, 2H, J = 5.9 Hz), 8.17 - 8.86 (m, 5H), 10.18 (d, 1H, J = 7.2 Hz). FABMS (M^+) : $C_{15}H_{18}NO_2$; found : 244.

Compound 1c. The benzothiazole derivatized product **1b**[15] (2.44 g, 7.54 mmoles) was added in one portion to a vigorously stirred mixture of **1a** (2.55 g, 7.54 mmoles) dissolved in 20 mL of warm EtOH. Et_3N (0.763 g, 7.54 mmoles) was addded dropwise, and the mixture was stirred at room temperature for 30 min, and at 60°C for another 30 min. After cooling to room temperature, 40 mL of ether was added to the mixture. The precipitate formed was collected by filtration, washed with ether, and dried *in vacuo* to afford the product **1c** in 74% yield. ^{1}H-NMR (in $CDCl_3$, 500 MHz) δ = 1.29 (t, 3H, J = 6.7 Hz), 2.92 (t, 2H, J = 5.5 Hz), 4.07 (s, 3H), 4.18 (q, 2H, J = 6.9 Hz), 4.91 (t, 2H, J = 5.7 Hz), 6.70 (s, 1H), 7.33 - 8.08 (m, 8H), 8.54 (d, 1H, J = 3.5 Hz), 9.22 (d, 1H, J = 3.6 Hz). ^{13}C-NMR (in D_2O, 500 MHz) δ = 29.3, 33.0, 34.8, 55.5, 79.5, 110.9, 111.5, 115.8,

120.2, 120.7, 121.2, 121.4, 125.1, 126.4, 137.3, 138.8, 142.0, 143.4, 144.1, 147.5, 148.80, 177.4. HRMS found *m/z* 391.4425, calcd for $C_{23}H_{23}N_2SO_2$, 391.4480.

Compound 1. 1c (250 mg, 0.577 mmoles) was dissolved in 5 mL of 1:1 2N NaOH/dioxane mixture, and stirred at room temperature for 12 h. The mixture was acidified with 1M HCL, and evaporated to dryness. 10 mL of DMF was added to dissolve the dried precipitate, and the reaction mixture was immersed in an ice bath. 1-Hydroxybenzotriazole (HOBT, 0.117 g, 0.866 mmoles) and dicyclohexylcarboiimide (DCC, 0.179 g, 0.866 mmoles) were added and the mixture was vigorously stirred for 30 min. Paramomycin sulfate (1.776 g, 2.885 mmoles), dissolved in 2 ml of 10% $NaHCO_3$, was then added dropwise. The reaction mixture was stirred at room temperature for 12 h. 20 mL of water was added to the reaction mixture, and the solution was passed through an anion exchange column (CG50, Sigma), and washed with 150 mL of water and 150 mL of 0.025 M of ammonium hydroxide. The crude product 1 was eluted with 1.25 M ammonium hydroxide. This crude product was purified by HPLC on an ODS column with a gradient of acetonitrile and water. The acetonitrile concentration was increased from 0% to 40% over 40 min. All solvents contained 1% of trifluoroacetic acid. The isolated product (48% yield) was then concentrated *in vacuo* and lyopholized. ^{1}H-NMR (in D_2O, 500 MHz) ^{1}H-NMR (in D_2O, 500 MHz) δ = 1.68 (t, 1H, J = 3.5 Hz), 1.94 (d, 1H, J = 3.7 Hz), 2.33 (m, 1H), 2.68 (q, 1H, J = 3.6 Hz), 3.10 (dd, 1H, J = 3.4 Hz), 3.30 - 3.94 (m, majority), 4.21 (q, 1H, J = 3.6 Hz), 4.38 (s, 1H), 4.39 (t, 1H, J = 3.9 Hz), 4.43 (t, 1H, J = 3.6 Hz), 4.51 (m, 1H), 5.21 (d, 1H, J = 4.9 Hz), 5.49 (bs, 1H), 6.74 (s, 1H), 7.26 - 7.71 (m, 10H), 8.86 (d, 1H, J = 4.8 Hz), 8.93 (d, 1H, J = 4.0 Hz). ^{13}C-NMR (in D_2O, 500 MHz) δ = 29.5, 29.6, 33.5, 37.0, 40.1, 50.2, 51.5, 54.1, 57.8, 60.8, 60.9, 62.4, 66.4, 68.9, 73.2, 74.1, 74.5, 75.70, 76.3, 77.2, 78.1, 78.4, 79.1, 88.0, 103.8, 105.9, 111.6, 111.7, 117.6, 120.0, 120.1, 120.9, 121.6, 122.1, 125.8, 126.0, 136.9, 139.7, 142.9, 143.9, 144.8, 146.0, 149.6, 178.9. HRMS found *m/z* 960.4068, calcd for $C_{44}H_{62}N_7SO_{15}$, 960.4024.

Compound 2. ^{1}H-NMR (in D_2O, 500 MHz) δ = 1.41 (t, 1H, J = 3.8 Hz), 1.70 (t, 1H, J = 3.8 Hz), 2.30 (t, 1H, J = 3.7 Hz), 2.65 (m, 1H), 2.91 (q, 1H, J = 3.3 Hz), 3.17 (t, 1H, J = 3.2 Hz), 3.33 - 3.85 (m, majority), 4.59 (dd, 1H, J = 3.6 Hz), 4.65 (d, 1H, J = 3.6 Hz), 4.72 (t, 1H, J = 3.4 Hz), 4.88 (t, 1H, J = 3.8 Hz), 5.34 (d, 1H, J = 4.7 Hz), 5.41 (bs, 1H), 6.75 (s, 1H), 7.08 - 7.74 (m, 10H), 8.72 (d, 1H, J = 4.5 Hz), 8.84 (d, 1H, J = 4.6 Hz). ^{13}C-NMR (in D_2O, 500 MHz) δ = 27.5, 29.0, 29.6, 33.1, 36.9, 40.6, 49.8, 52.0, 55.0, 58.7, 59.1, 60.3, 63.1, 66.5, 69.2, 72.3, 73.8, 75.0, 76.9, 78.1, 78.7, 78.9, 79.3, 86.7, 100.3, 105.5, 111.3,

112.1, 112.9, 120.1, 120.8, 121.0, 121.4, 122.9, 125.1, 126.7, 136.6, 139.9, 142.3, 143.1, 143.8, 146.4, 148.4, 178.7. HRMS found *m/z* 975.4118, calcd for $C_{45}H_{65}N_7SO_{15}$, 975.4180. 51% yield.

Compound 3. ^{1}H-NMR (in D_2O, 500 MHz) δ = 1.40 (t, 1H, J = 3.7 Hz), 1.63 (t, 1H, J = 3.8 Hz), 1.69 (t, 2H, J = 3.7 Hz), 2.21 (m, 1H), 2.44 (t, 1H, J = 3.6 Hz), 3.01 (m, 1H), 3.28 - 3.76 (m, majority), 4.31 (q, 1H, J = 2.4 Hz), 4.53 (br, s, 1H), 4.56 (d, 1H, J = 4.3 Hz), 4.87 (t, 1H, J = 3.7 Hz), 4.91 (t, 1H, J = 3.6 Hz), 5.44 (d, 1H, J = 3.5 Hz), 5.56 (bs, 1H), 6.87 (s, 1H), 7.12 - 7.90 (m, 10H), 8.77 (d, 1H, J = 4.6 Hz), 9.21 (d, 1H, J = 4.3 Hz). ^{13}C-NMR (in D_2O, 500 MHz) δ = 28.4, 29.4, 29.8, 30.3, 32.0, 36.4, 42.1, 48.9, 50.3, 54.9, 56.8, 59.5, 61.4, 63.0, 65.3, 69.2, 71.2, 73.7, 74.1, 76.4, 77.2, 78.7, 78.9, 79.0, 82.1, 98.4, 105.0, 109.1, 110.6, 111.3, 112.0, 119.9, 120.2, 121.1, 121.7, 122.4, 123.8, 127.0, 133.5, 137.9, 141.8, 142.8, 144.5, 147.2, 147.7, 175.3. HRMS found *m/z* 988.4364, calcd for $C_{46}H_{66}N_7SO_{15}$, 988.4337. 42% yield.

Compound 4. ^{1}H-NMR (in D_2O, 500 MHz) δ = 1.32 (t, 2H, J = 2.9 Hz), 1.51 (t, 2H, J = 3.3 Hz), 1.54 (m, 1H), 1.69 (m, 2H), 1.94 (m, 2H), 2.34 (m, 2H), 2.43 (m, 1H), 2.88 (t, 1H, J = 3.0 Hz), 3.07 (t, 1H, J = 2.9 Hz), 3.32 - 3.94 (m, majority), 4.21 (m, 1H), 4.35 (s, 1H), 4.25 (d, 1H, J = 4.2 Hz), 4.43 (t, 1H, J = 3.4 Hz), 4.52 (t, 1H, J = 3.5 Hz), 5.21 (d, 1H, J = 4.3 Hz), 6.73 (s, 1H), 7.11 - 7.78 (m, 10H), 9.07 (d, 1H, J = 4.4 Hz), 9.25 (d, 1H, J = 4.5 Hz). ^{13}C-NMR (in D_2O, 500 MHz) δ = 27.1, 28.3, 28.8, 29.0, 29.5, 34.7, 39.7, 44.6, 48.9, 50.4, 53.9, 55.2, 58.3, 60.3, 61.4, 681, 68.6, 72.1, 73.8, 76.2, 78.0, 78.3, 78.4, 78.5, 78.7, 79.0, 86.1, 100.4, 104.7, 111.9, 112.6, 112.9, 120.7, 120.9, 121.5, 121.6, 123.6, 126.0, 126.7, 134.4, 136.8, 140.9, 142.6, 144.3, 147.7, 147.9, 176.1. HRMS found *m/z* 1002.4467, calcd for $C_{47}H_{68}N_7SO_{15}$, 1002.4493. 45% yield.

Compound 5. ^{1}H-NMR (in D_2O, 500 MHz) δ = 1.24 (t, 2H, J = 3.4 Hz), 1.48 (t, 2H, J = 3.3 Hz), 1.55 (t, 2H, J = 3.5 Hz), 1.79 (t, 2H, J = 3.5 Hz), 2.43 (m, 1H), 2.88 (q, 1H, J = 2.8 Hz), 3.10 (t, 1H, J = 3.5 Hz), 3.30 - 3.93 (m, majority), 4.21 (q, 1H, J = 3.0 Hz), 4.38 (br, s, 1H), 4.39 (d, 1H, J = 3.9 Hz), 4.43 (t, 1H, J = 3.7 Hz), 4.51 (t, 1H, J = 3.5 Hz), 5.22 (d, 1H, J = 4.0 Hz), 5.49 (bs, 1H), 6.74 (s, 1H), 7.26 - 7.71 (m, 10H), 8.86 (d, 1H, J = 4.2 Hz), 8.90 (d, 1H, J = 4.3 Hz). ^{13}C-NMR (in D_2O, 500 MHz) δ = 28.7, 28.8, 29.1, 29.2, 30.5, 30.9, 35.0, 38.7, 43.4, 51.7, 51.9, 55.0, 58.9, 61.8, 62.4, 63.9, 68.1, 69.9, 74.1, 75.0, 75.2, 76.4, 77.0, 78.3, 79.1, 79.5, 79.8, 89.8, 100.6, 106.3, 110.8, 111.4, 111.8, 118.7, 120.9, 121.5, 122.0, 122.6,

124.7, 129.3, 134.2, 140.1, 141.8, 142.7, 143.1, 144.5, 146.7, 173.7. HRMS found *m/z* 1016.4618, calcd for $C_{48}H_{70}N_7SO_{15}$, 1016.4650. 50% yield.

Synthesis of the Paramomycin-Pyrene Conjugates. The general synthetic procedures for the various paramomycin-pyrene conjugates are similar. Hence, only the synthetic procedures for only pyrenecarbonyl labeled paramomycin (PCP, **6**) will be described in detail.

Compound 6. To a solution of pyrenecarboxylic acid (50 mg, 0.203 mmoles) dissolved in DMF, DCC (41.9 mg, 0.203 mmoles) was added and stirred for 1 h. N-Hydroxysuccinimide (23.36 mg, 0.203 mmoles) was added to the reaction and stirred for 1 h. A solution of paramomycin (624 mg, 1.105 mmoles), dissolved in 2:1 DMF / water, was added dropwise to the reaction mixture and stirred for 12 h at room temperature. The solution was evaporated, and the crude product was first purified by Sephadex CM-25 ion-exchange column chromatography, followed by HPLC equipped with a semi-preparative Dynamax C18 column. The acetonitrile concentration was increased from 0% to 40% over 40 min. All solvents contained 1% of trifluoroacetic acid. The isolated product of PCP (63% yield) was then concentrated *in vacuo* and lypholized. ^{1}H-NMR (in D_2O, 500 MHz) δ = 1.61 (t, 1H, J = 4.3 Hz), 2.34 (m, 1H), 2.88 (q, 1H, J = 3.7 Hz), 3.10 (t, 1H, J = 3.7 Hz), 3.30 - 3.94 (m, majority), 4.21 (q, 1H, J = 3.9 Hz), 4.38 (s, 1H), 4.39 (d, 1H, J = 4.4 Hz), 4.43 (t, 1H, J = 4.4 Hz), 4.51 (t, 1H, J = 4.5 Hz), 5.22 (d, 1H, J = 4.7 Hz), 5.49 (bs, 1H), 8.32 - 8.49 (m, 9H). ^{13}C-NMR (in D_2O, 500 MHz) δ = 28.8, 30.0, 40.6, 48.6, 53.6, 56.8, 59.3, 60.0, 61.4, 64.7, 66.1, 70.1, 72.5, 72.9, 75.3, 76.6, 77.8, 78.2, 78.9, 80.1, 83.5, 100.4, 104.9, 113.6, 120.3, 123.9, 124.4, 125.8, 127.1, 128.6, 128.8, 129.1, 129.2, 129.4, 130.1, 130.5, 134.7, 136.6, 143.0, 179.0. HRMS found *m/z* 843.3588, calcd for $C_{40}H_{54}N_5O_{15}$, 843.3537.

Compound 7. ^{1}H-NMR (in D_2O, 500 MHz) δ = 1.70 (t, 1H, J = 3.7 Hz), 2.05 (s, 2H), 2.42 (m, 1H), 2.75 (q, 1H, J = 4.0 Hz), 3.13 (m, 2H), 3.56 (t, 1H, J = 4.2 Hz), 3.32 - 4.10 (m, majority), 4.32 (q, 1H, J = 3.8 Hz), 4.48 (br, s, 1H), 4.65 (d, 1H, J = 4.3 Hz), 4.74 (t, 1H, J = 3.7 Hz), 4.89 (t, 1H, J = 3.6 Hz), 5.37 (d, 1H, J = 4.2 Hz), 5.59 (bs, 1H), 8.34 - 8.52 (m, 9H). ^{13}C-NMR (in D_2O, 500 MHz) δ = 29.4, 29.6, 36.5, 42.7, 48.6, 50.8, 56.8, 60.1, 61.8, 62.1, 67.5, 69.5, 72.1, 73.7, 75.2, 76.9, 77.4, 78.6, 78.8, 79.07, 79.9, 87.2, 100.4, 105.7, 118.3, 120.6, 123.0, 124.9, 126.1, 126.8, 127.3, 128.0, 128.4, 128.9, 129.5, 132.7, 133.5, 136.2, 136.6, 148.9, 176.1. HRMS found *m/z* 857.3602, calcd for $C_{41}H_{56}N_5O_{15}$, 857.3694. 58% yield.

Compound 8. ^{1}H-NMR (in D_2O, 500 MHz) δ = 1.41 (m, 2H), 1.55 (q, 1H, J = 3.9 Hz), 12.31 (m, 2H), 2.65 (m, 1H), 2.79 (m, 2H), 2.95 (q, 1H, J = 4.2 Hz), 3.15 (t, 1H, J = 3.8 Hz), 3.32 - 3.94 (m, majority), 4.21 (q, 1H, J = 4.0 Hz), 4.38 (br, s, 1H), 4.39 (d, 1H, J = 4.7 Hz), 4.43 (t, 1H, J = 4.4 Hz), 4.51 (t, 1H, J = 4.5 Hz), 5.22 (d, 1H, J = 4.5 Hz), 5.49 (bs, 1H), 8.32 - 8.49 (m, 9H). ^{13}C-NMR (in D_2O, 500 MHz) δ = 29.5, 29.6, 29.7, 33.4, 37.0, 40.0, 50.0, 51.2, 57.2, 60.2, 60.9, 62.6, 66.6, 68.5, 73.5, 74.6, 74.8, 77.5, 77.8, 78.1, 78.6, 78.7, 79.6, 86.0, 102.6, 108.3, 116.8, 121.8, 124.7, 125.0, 126.5, 126.7, 127.1, 127.4, 127.6, 128.1, 129.4, 131.4, 131.4, 135.2, 135.9, 144.2, 175.6. HRMS found *m/z* 885.4049, calcd for $C_{43}H_{60}N_5O_{15}$, 885.4007. 62% yield.

Compound 9. ^{1}H-NMR (in D_2O, 500 MHz) δ = 1.39 (m, 2H), 1.47 (m, 2H), 1.51 (m, 2H), 1.56 (t, 1H, J = 3.9 Hz), 1.86 (dd, 2H), 2.43 (m, 2H), 2.45 (m, 1H), 2.54 (m, 2H), 2.93 (q, 1H, J = 3.5 Hz), 3.14 (t, 1H, J = 3.6 Hz), 3.40 - 4.12 (m, majority), 4.24 (q, 1H, J = 3.8 Hz), 4.40 (br, s, 1H), 4.43 (d, 1H, J = 4.5 Hz), 4.65 (t, 1H, J = 4.5 Hz), 4.74 (t, 1H, J = 4.5 Hz), 5.43 (d, 1H, J = 4.8 Hz), 5.52 (bs, 1H), 8.32 - 8.49 (m, 9H). ^{13}C-NMR (in D_2O, 500 MHz) δ = 28.6, 29.0, 29.5, 29.8, 31.6, 34.5, 36.4, 39.9, 48.6, 50.7, 55.4, 58.7, 59.4, 60.91, 65.1, 67.4, 71.1, 72.1, 73.8, 76.9, 78.0, 78.6, 78.8, 78.8, 80.7, 87.5, 100.5, 107.8, 114.6, 119.3, 122.8, 124.8, 125.0, 126.1, 126.8, 126.9, 127.3, 127.4, 128.2, 130.1, 132.8, 134.6, 136.4, 142.9, 178.8. HRMS found *m/z* 914.4351, calcd for $C_{45}H_{64}N_5O_{15}$, 913.4320. 61% yield.

Compound 10. ^{1}H-NMR (in D_2O, 500 MHz) δ = 1.37 (m, 2H), 1.55 (m, 2H), 1.60 (dd, 2H, J = 3.5 Hz), 1.61 (m, 2H), 1.67 (m, 2H), 1.72 (m, 2H), 1.73 (t, 1H, J = 3.8 Hz), 2.40 (m, 1H), 2.82 (q, 1H, J = 3.4 Hz), 3.12 (t, 1H, J = 3.7 Hz), 3.33 - 3.94 (m, majority), 4.20 (q, 1H, J = 4.3 Hz), 4.36 (br, s, 1H), 4.39 (d, 1H, J = 3.8 Hz), 4.41 (t, 1H, J = 4.0 Hz), 4.50 (t, 1H, J = 3.8 Hz), 5.17 (d, 1H, J = 4.0 Hz), 5.53 (bs, 1H), 8.46 - 8.52 (m, 9H). ^{13}C-NMR (in D_2O, 500 MHz) δ = 29.0, 29.3, 29.5, 29.5, 29.6, 29.8, 29.9, 30.6, 31.6, 32.5, 36.7, 38.7, 47.3, 48.8, 55.1, 58.2, 60.2, 63.6, 67.4, 69.9, 72.2, 73.9, 75.6, 76.0, 76.9, 77.6, 78.0, 78.6, 79.6, 85.5, 100.4, 104.9, 113.7, 119.0, 123.3, 126.0, 126.7, 126.8, 127.0, 127.8, 128.0, 128.3, 129.1, 130.9, 133.2, 134.9, 135.3, 140.6, 177.3. HRMS found *m/z* 969.4933, calcd for $C_{49}H_{71}N_5O_{15}$, 969.4946. 56% yield.

Fluorescence Measurements. Fluorescence measurements were performed on a LS-50B spectrofluorometer (Perkin-Elmer) at 20.0 ± 0.1°C in the selection buffer (140 mM NaCl, 5 mM KCl, 1 mM $CaCl_2$, 1 mM $MgCl_2$ and 20 mM HEPES (pH = 7.4)) as previously described[9,10].

REFERENCES

(1) Chow, C.; Bogdan, F. M. *Chem. Rev.* **1997**, 97, 1489-1513; and references therein.

(2) (a) von Ashen, U.; Davies, J.; Schreoder, R. *Nature* **1991**, 353, 368-370. (b) von Ashen, U.; Davies, J.; Schreoder, R. *J. Mol. Biol.* **1992**, 226, 935-941. (c) Stage, T. K.; Hertel, K. J.; Uhlenbeck, O. C. *RNA* **1995**, 1, 95-101. (d) Zapp, M. L.; Stern, S.; Green, M. R. *Cell* **1993**, 74, 969-978.

(3) Hutchin, T.; Haworth, I.; Higashi, K.; Fischel-Ghodsian, N.; Stoneking, M.; Saha, N.; Amos, C.; Cortopassi, G. *Nucleic Acid Res.* **1993**, 21, 4174-4179.

(4) (a) Cundliffe, E. *Annu. Rev. Micro.* **1989**, 43, 207-233. (b) Cundliffe, E. In *The Ribosome: Structure, Function & Evolution.* (Hill, W. E., Dahlberg, A. E., Garrett, R. A., Moore, P. B., Schlessinger, D. & Warner, J. R., eds), **1990**, 479-490, American Society for Microbiology, Washington, D.C.

(5) (a) Gale, E. F.; Cundliffe, E.; Reynolds, P. E.; Richmond, M. H.; Waring, M. J. *The Molecular Basis of Antibiotic Action* (2nd ed.) **1981**, 419-439, John Wiley & Sons, London, Great Britain. (b) Chambers, H. F. & Sande, M. A. *The Aminoglycosides* (Hardman, J. G., Limbird, L. E., Molinoff, P. B., Ruddon, R. W., & Goodman Gilman, A., Eds.) in Goodman & Gilman's *The Pharmacological Basis of Therapeutics* (9th ed.) **1996**, Chapter 46, 1103-1121, McGraw-Hill, New York.

(6) (a) Moazed, D.; Noller, H. F. *Cell* **1986**, 47, 985-994. (b) Moazed, D.; Noller, H. F. *Nature* **1987**, 327, 389-394. (c) Moazed, D.; Noller, H. F. *J. Mol. Biol.* **1990**, 211, 135-145. (d) Woodcook, J.; Mozaed, D.; Cannon, M.; Davies, J.; Noller, H. F. *EMBO J.* **1991**, 10, 3099-3103.

(7) Purohit, P.; Stern, S. *Nature* **1994**, 370, 659-662.

(8) (a) Fourmy, D.; Recht, M. I.; Blanchard, S. C.; Puglisi, J. D. *Science* **1996**, 274, 1367-1371. (b) Recht, M. I.; Fourmy, D.; Blanchard, S. C.; Dahlquist, K. D.; Puglisi, J. D. *J. Mol. Biol.* **1996**, 262, 421-426.

(9) Wang, Y.; Hamasaki, K.; Rando R. R. *Biochemistry* **1997**, 36, 768-779.

(10) (a) Wang, Y.; Rando R. R. *Chem. Biol.* **1996**, 2, 281-290. (b) Wang, Y.; Killian, J.; Hamasaki, K.; Rando R. R. *Biochemistry* **1996**, 35, 12338-12346.

(11) (a) Appel, G. B.; Neu, H. C. *N. Engl. J. Med.* **1977**, 296, 722-728. (b) Harpur, E. *Brit. J. Aud.* **1982**, 16, 81-93.

(12) Hamasaki, K.; Rando, R. R. *Biochemistry* **1997**, 36, 12323-12328.

(13) (a) Benecky, M. J.; Wine, R. W.; Kolvenbach, C. G.; Mosesson, M. W. *Biochemistry* **1991**, 30, 4298-4306. (b) Fritzsche, H.; Akhebat, A.; Taillander, E.; Rippe, K.; Jovin, T. *Nucleic Acid Res.* **1993**, 21, 5085-5091.

(14) (a) Jacobsen, J. P.; Pederson, J. B.; Hansen L. F.; Wemmer, D. E. *Nucleic Acid Res.* **1995**, 23, 753-760. (b) Hansen, L. F.; Jensen, L. K.; Jacobsen, J. P. *Nucleic Acid Res.* **1996**, 24, 859-867. (c) Faridi, J.; Nielsen, K. E.; Stein, P. C.; Jacobsen, J. P. *J. Bimolecular Struc. & Dynamics.* **1997**, 15, 321-332.

(15) (a) Rye, H. S.; Yue, S.; Wemmer, D. E.; Quesada, M. A.; Haugland, R. P.; Mathies, R. A.; Glazer, A. N. *Nuclei Acid Res.* **1992**, 20, 2803-2812. (b) Benson, S. C.; Singh, P.; Glazer, A. N. *Nuclei Acid Res.* **1993**, 21, 5727-5735. (c) Rye, H. S.; Glazer, A. N. *Nucleic Acid Res.* **1995**, 23, 1215-1222.

(16) Pilch, D. S.; Kirolos, M. A.; Liu, X.; Plum, G. E.; Breslauer, K. J. *Biochemistry* **1995**, 34, 9962-9976.

(17) Tanious, F. A.; Veal, J. M.; Buczak, H.; Ratmeyer, L. S.; Wilson, W. D. *Biochemistry* **1992**, 31, 3103-3112.

(18) Zhao, M.; Janda, L.; Nguyun, J.; Strekowski, L.; Wilson, W. D. *Biopolymers* **1994**, 34, 61-73.

(19) (a) Ratmeyer L.; Zapp, M. L.; Green, M. R.; Vinayak, R.; Kumar, A.; Boykin, D. W.; Wilson, W. D. *Biochemistry* **1996**, 35, 13689-13696. (b) Zapp, M. L.; Young, D. W.; Kumar, A.; Singh, R.; Boykin, D. W.; Wilson, W. D.; Green, M. R. *Biorganic & Med. Chem.* **1997**, 5, 1149-1155.

(20) (a) McConnaughie, A. W.; Spychala, J.; Zhao, M.; Boykin, D.; Wilson, W. D. *J. Med. Chem.* **1994**, 37, 1063-1069. (b) Bailly, C.; Colson, P.; Houssier, C.; Hamy, F. *Nucleic Acids Res.* **1996**, 24, 1460-1464. (c) Bourdouxhe, C.; Colson, P.; Houssier, C.; Sun, J. S.; Montenay-Garestein, T.; Helene, C.; Rivalle, C.; Bisagni, E.; Waring, M. J.; Henichart, J-P.; Bailly, C. *Biochemistry* **1992**, 31, 12385-12396. (d) Bailly, C.; D'Huigin, C.; Houssin, R.; Colson, P.; Houssier, C.; Rivalle, C.; Bisagni, E.; Henichart, J-P.; Waring, M. *J. Mol. Pharm.* **1992**, 41, 845-855.

(21) (a) Ratmeyer, L. S.; Vinayak, R.; Zon, G.; Wilson, W. D. *J. Med. Chem.* **1992**, 35, 966-968. (b) Wilson, W. D.; Ratmeyer L.; Cegla, M. T.; Spychala, J.; Boykin, D.; Demeunynck, M.; Lhomme, J.; Krishnan, G.; Kennedy, D.; Vinayak, R.; Zon, G. *New J. Chem.* **1994**, 18, 419-426.

ACKNOWLEDGMENT

We gratefully acknowledge the input and stimulating discussion from the members of the laboratory. The work was partially supported by U.S. Public Health Service National Institutes of Health Grants EY-03624 and EY-04096.